

***AutArch*: An AI-assisted workflow for object detection and automated recording in archaeological catalogues**

Kevin Klein^{1,2*}, Alyssa Wohde³, Alexander V. Gorelik^{1,2}, Volker Heyd⁴, Yoan Diekmann^{1#},
Maxime Brami^{1#*}

These authors contributed equally.

* Corresponding authors: Kevin Klein (kkevin@students.uni-mainz.de), Maxime Brami (mbrami@uni-mainz.de)

Affiliation

¹Palaeogenetics Group, Institute of Organismic and Molecular Evolution (iomE), Johannes Gutenberg University Mainz, Mainz, Germany.

²Vor- Und Frühgeschichtliche Archäologie, Institut Für Altertumswissenschaften, Johannes Gutenberg University Mainz, Mainz, Germany.

³University of Koblenz, Koblenz, Germany

⁴Department of Cultures / Archaeology, University of Helsinki, Helsinki, Finland

Abstract

Compiling large datasets from published resources, such as archaeological find catalogues presents fundamental challenges: identifying relevant content and manually recording it is a time-consuming, repetitive and error-prone task. For the data to be useful, it must be of comparable quality and adhere to the same recording standards, which is hardly ever the case in archaeology. Here, we present a new data collection method exploiting recent advances in Artificial Intelligence. Our software uses an object detection neural network combined with further classification networks to speed up, automate, and standardise data collection from legacy resources, such as archaeological drawings and photographs in large unsorted PDF files. The AI-assisted workflow detects common objects found in archaeological catalogues, such as graves, skeletons, ceramics, ornaments, stone tools and maps, and spatially relates and analyses these objects on the page to extract real-life attributes, such as the size and orientation of a grave based on the north arrow and the scale. A graphical interface allows for and assists with manual validation. We demonstrate the benefits of this approach by collecting a range of shapes and numerical attributes from richly-illustrated archaeological catalogues, and benchmark it in a real-world experiment with ten users. Moreover, we record geometric whole-outlines through contour detection, an alternative to landmark-based geometric morphometrics not achievable by hand.

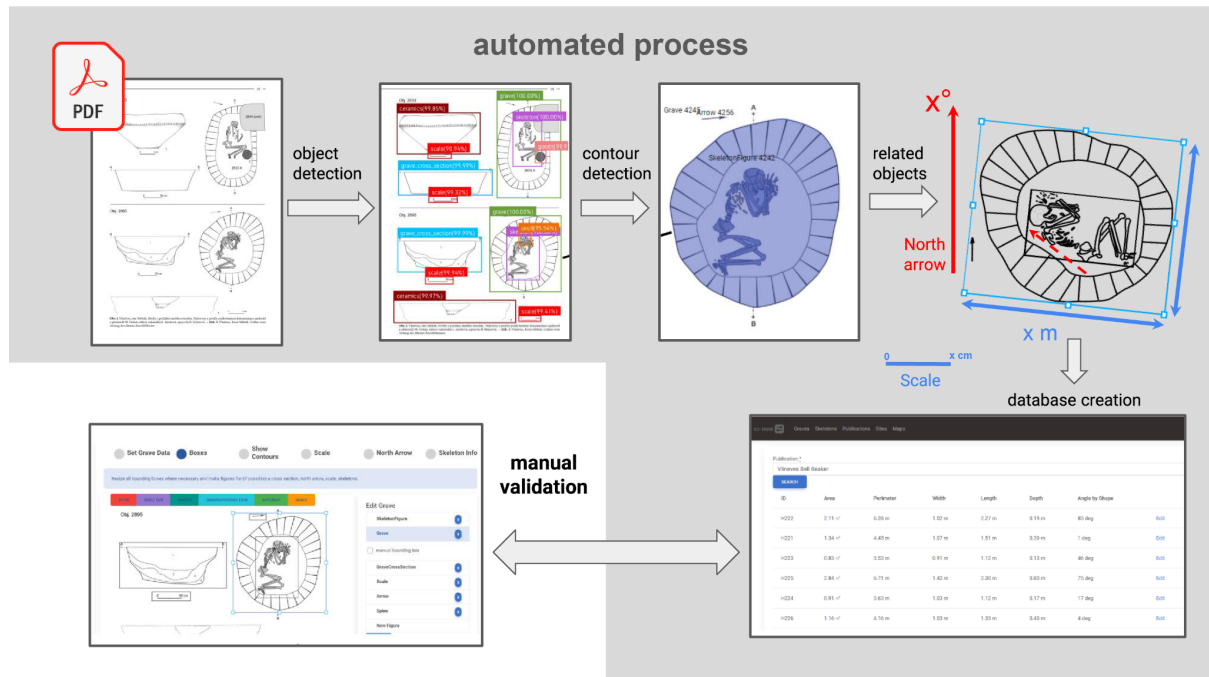
Keywords

Archaeology, Artificial Intelligence (AI), Object Detection, Deep Learning, Geometric Morphometrics

Highlights

- Automating archaeological data collection using legacy resources
- Fast and standardised recording for Big Data archaeology
- Contour detection and encoding allowing formal analyses of shapes

Graphical Abstract



Graphical Abstract. Overview of the AI-assisted workflow (here: Corded Ware site of Vliněves¹, Czech Republic).

Video

A video demonstrating the key aspects of the software can be downloaded at this address:

<https://seafire.rlp.net/f/50ce9cc0771f4afc9cd0/>

1.1 Introduction

Big data and archaeology: towards an AI solution

The use of Artificial Intelligence and Big Data models in scientific and commercial applications surged in popularity in recent years. Advances in deep learning, for instance, have enabled users to solve complex image processing problems. These new approaches are often argued to be the next frontier ² in archaeology, with multiple attempts to consolidate all archaeological datasets into single databases already on the way (e.g. Big Interdisciplinary Archaeological Database or BIAD: <https://biadwiki.org/>).

While the benefits of integrating information from thousands of archaeological PDFs released to date are obvious, there are significant hurdles. Screening thousands of pages of text and images to locate relevant content is a time-consuming and repetitive task; data can be scattered across many parts of the document; papers can be written in different languages and alphabets; various conventions for describing attributes such as the size and orientation of graves apply, so that mere collation of data from published tables results in inconsistent datasets. Using Computer-Assisted Design (CAD) or drawing software products to manually re-measure objects based on published drawings is tedious and prone to error. Therefore, large-scale assembly of consistent and error-free data from a variety of sources is rarely possible in practice.

Especially the lack of unified drawing standards in archaeology complicates data comparison across publications. Measuring the width, length and depth of a three-dimensional object, such as a burial pit, for instance, might be expected to yield consistent results independent of author and publication; yet, there are multiple ways to describe objects in archaeology, particularly for irregular shapes. Archaeological site manuals ³ rarely provide guidelines on how to measure non-symmetrical objects such as graves. And while some authors show how the length was measured by drawing a line through the grave e.g. ^{4,5}, the width is rarely indicated in the same manner. Even if this information was transparently reported, harmonising measurement conventions would remain a challenge. Reporting the orientation of skeletons in graves is fraught with even more difficulties ⁶. The orientation of graves is rarely given in degrees, and when it is, different methods are applied, often confusing the orientation of the skeleton with the orientation of the grave cut. In sum, there is no guarantee that reported measurements of spatial objects can be compared across different publications.

In this paper, we present *AutArch*, an AI-assisted workflow that allows fast, accurate, and consistent identification and analysis of objects in unsorted PDF documents. Previous archaeological approaches leveraging AI have often addressed narrowly focused research questions, e.g. classification of artefacts and ecofacts ^{7–11}, predicting the dating of sites ¹², or interpretation of high-resolution survey images ^{13–15}. Despite archaeology's emphasis since the 19th century on typological and geometric morphometric approaches ¹⁶, published resources such as archaeological drawings and photographs in illustrated catalogues have remained underutilised ¹⁷. The process of extracting geometric shapes from publications is starting to be semi-automated for specific artefact classes, such as arrowheads, but the images still need to be prepared for the extraction of artefact outlines ^{18,19}. *AutArch* provides a general solution that increases the usefulness of published resources by making their content immediately available to archaeology as data in a well-defined format.

Background to the Research

Due to the ‘messy’²⁰, but to some extent repetitive nature of the archaeological record in third millennium BC Europe, this period provides an interesting testing ground for innovative approaches using AI. Tens of thousands of graves and grave inventories have been ascribed to this period. The findings are frequently reported in the form of drawings and photographs accompanied by descriptions written following a variety of professional standards and in different languages. Historically, archaeological assemblages have been grouped into archaeological ‘cultures’, based on different classes of attributes, making comparison difficult. Southeast European ‘Yamnaya’ assemblages, for instance, are defined after a specific type of burial, i.e. ‘pit-graves’^{21,22}; North-Central European ‘Corded Ware’ assemblages are characterised by a specific ceramic decoration²³; Western European ‘Bell Beakers’ are named after the shape of the ceramic vessels found in graves^{24,25}. These attributes sometimes appear together. For instance, All Over Cord (AOC) Beakers have cord impressions²⁶. While many studies have dealt with variability in the funerary record, most are still based on the simplest possible attribute dimension, its presence or absence. The challenge is to develop an automated workflow that requires only minimal input from researchers to digitise large datasets recording rich, numerical annotation.

1.2 Materials and Methods

We present an AI-assisted tool that processes data in the form of illustrations found in archaeological publications to automatise the measurement and comparison of typological attributes. In this manner, our approach provides a way to collect, analyse and compare archaeological data in an objective way.

Dataset

As primary dataset, we used catalogues of 3rd millennium BCE graves, which we manually annotated for object detection using *labelImg* (<https://github.com/HumanSignal/labelImg>). In total, 391 pages were annotated (**table 1**). The quality and detail of the annotated material range from high-resolution digital catalogues, such as those published for the sites of Vliněves in the Czech Republic^{1,27}, to lower-quality book scans and even hand-drawn notes from Southeast European and Russian excavations. The corresponding archaeological sites are shown in **figure 1**.

Each page of these documents was converted to an image and randomly sampled. Initially we annotated all pages with drawings from four publications^{1,27–29}. For the extended dataset a random sample was used and a manual selection was done to maximise the number of pages containing relevant drawings.

Class label	Object Count
text	850
skeleton photo	52
ceramics	615
artefact	535
grave photo	122

map	59
scale	905
arrow	532
grave	376
skeleton	404
grave artefact	207
grave cross section	240
stone tool	346
shaft axe	121

Table 1. Number of annotated objects in the primary dataset per class.

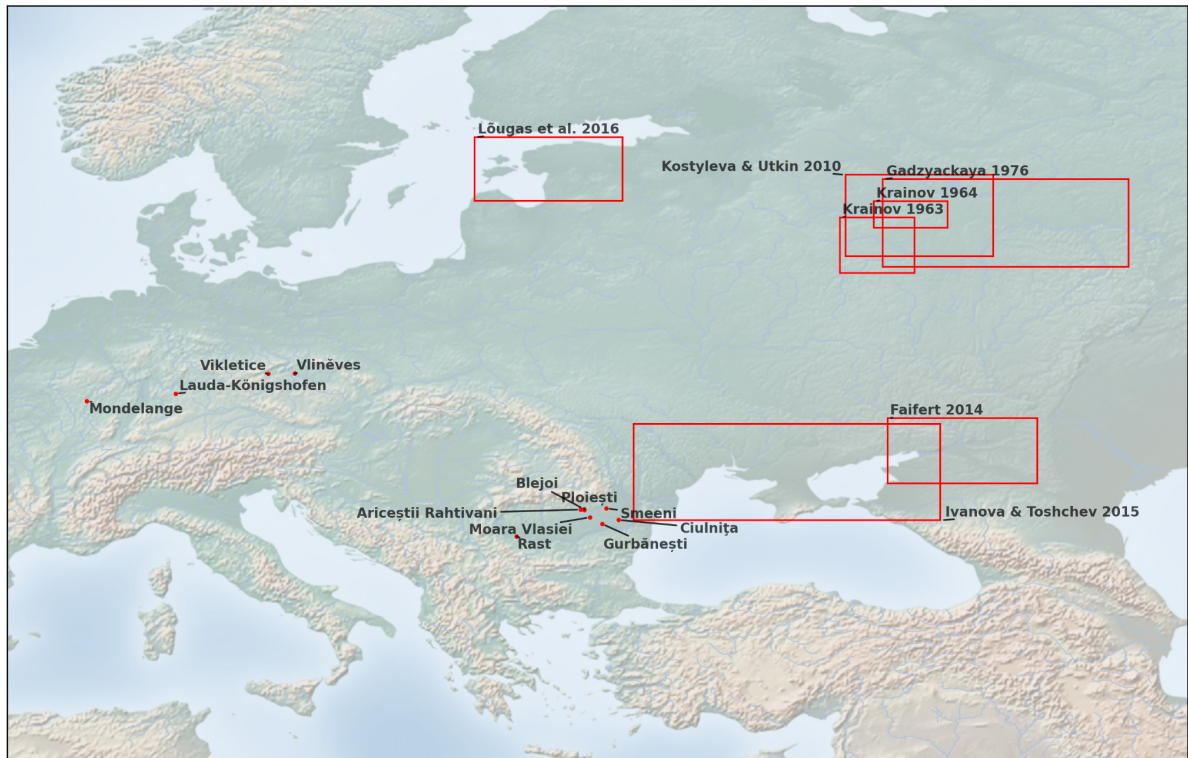


Figure 1. Map of sites used in training and/or validation (drawn with Matplotlib Basemap Toolkit 1.3.8 and Python 3.11; background is a display shaded relief image from <http://www.shadedrelief.com>).

Automated Step

Our software relies on Deep Learning (DL) for object detection, which is a type of artificial neural network (ANN). ANNs are mathematical function networks that can be thought of as layers of artificial neurons (also known as Perceptrons or Nodes). Neurons have one or several inputs with associated weights, a bias- and an activation function. For simple linear layers, each input is multiplied with its weight, the weighted inputs are summed, and the bias is added to it. The resulting

value is the argument of the activation function. Evaluating the function gives the final result that is passed onto the next layer which performs its calculations based on the output of the previous layer. Bias and input weights are the model parameters that need to be trained given annotated input data. For example, our software extensively uses Resnet-152 (Residual Neural Network), which has a total of 115.6 million parameters ³⁰.

Aside from linear layers, other common layer types include convolutional layers, which reduce multidimensional data (commonly 1, 2 or 3) to scalars, and pooling layers, which are similar to convolutional layers but do not have parameters that need to be trained.

In image processing, two types of neural networks with different purposes are commonly used: object detection, and classification. Classification assigns an object (such as an image of a skeleton) to a predefined number of labelled classes (such as ‘supine’ or ‘flexed on left side’ to describe the pose of the skeleton in the grave). Object detection networks, on the other hand, output a list of bounding boxes with a label for each of them. Each bounding box corresponds to a specific object detected in the image.

Models need to be trained to accurately perform the desired task. For supervised training of a model one needs a training dataset, a loss function and an optimiser. In our case, the training dataset consists of images of objects that were manually labelled and that the algorithm learns to recapitulate. Optimisers are algorithms that are executed on the model and tweak its parameters to improve classification accuracy, or in other words, that increase the number of times that given an image the correct label is produced. A loss function is used to quantify the prediction error, that is related to how often the model predicts incorrect labels. The output of an image classification network are the probabilities with which an object belongs to the different labelled classes (**figure 2**). For classification, a widely used loss function ³¹ is cross entropy loss, defined as

$$l(x, y) = - \sum_{c \in C} x(c) \log y(c), \text{ where } C \text{ is the set of classes and } x, y \text{ the predicted and true}$$

probability vector, respectively. Training a model on the whole dataset once is referred to as an “epoch”. Usually models are trained for hundreds or thousands of epochs to get a satisfying result. The training data is re-shuffled randomly before every training epoch to avoid learning effects caused by a specific order.

We use two different types of models in our application, Faster R-CNN (region-based convolutional neural network) ³², an object detection network here with MobileNetV3-Large 34 as its so-called backbone, and Resnet (residual neural network) ³³.

<i>label1</i>	72%
<i>label1</i>	12%
<i>label2</i>	16%

Figure 2. Probability for different labels.

All the documents we used for this project were in PDF format. The uploaded documents were saved to a database and converted to separate images for each page. These images were then scaled and fed into an R-CNN, trained with a set of archaeological drawings. Here the “Faster R-CNN” variety is used, which improves over the previous R-CNN and “Fast R-CNN” amongst others by a region proposal network and anchor boxes.

The result is a list of bounding boxes with labels for each page. These labels include “grave”, “skeleton”, “scale” and “north arrow” among others. These bounding boxes encapsulate the relevant object as shown on the page (**figure 3**). However, on their own the objects are not useful. Different types of objects have to be combined to represent entities interpretable by archaeologists, and allow

for metric measurements. Concretely, this means that graves have to be connected with their respective scales, north arrows, cross sections, artefacts and possible skeletons contained within the grave. We achieve this with a tree data structure.

To create fully annotated graves, the algorithm first combines all graves on a page. The nearest north arrow, scale and cross-section are assigned to each grave, using the Euclidean distance measured from the centre of the bounding boxes. These objects can be assigned to multiple graves at the same time. All skeletons and artefacts within the bounding box of the grave are then assigned to it.

Scales have to be further processed to parse the information they encode. For this, we devised a bespoke method using the contours of the bounding box detected using the OpenCV 4.6 implementation of *findContours* (based on Suzuki et al. ³⁴), and OCR (optical character recognition) with Tesseract (<https://github.com/tesseract-ocr/tesseract>). The contour analyser calculates the length of the scale while the OCR determines the factor for conversion from pixels into real-world distance.

The north arrows are analysed using a Resnet-152³³ residual neural network that retrieves their angle. Resnet consists mostly of stacked convolutional layers, which is a common architecture for image classification networks, and represents a significant improvement over previous networks mostly as it introduced shortcut connections. This network has been trained in an unsupervised manner as opposed to other neural networks discussed here. 118 north arrows (224x224 px) that have been rotated to point towards 0° degrees have been assembled. For every training step, those arrows are rotated by a random angle within 10° degree steps (0°, 10°, 20°, 30° ...). The rotated image is then processed by the neural network which predicts those 10° degree bins as a label. RMSProp³⁵ (root mean square propagation) was used as the optimizer with a learning rate of 1e-3. It was trained for 1000 epochs with a batch size of 16.

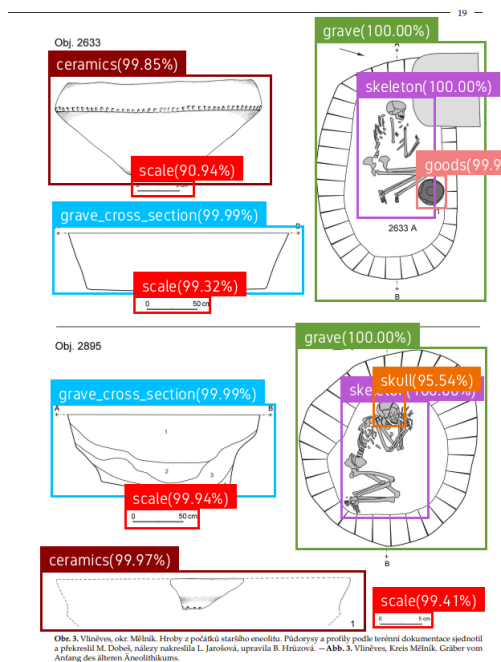


Figure 3. Example of the object detection result for one page of catalogue (here: Corded Ware site of Vlněves¹, Czech Republic). North arrows excluded for better visibility.

The size of a grave is measured by fitting a rotated rectangle minimising its area bounded by the outside of the contour³⁶. The width is assigned as the shorter side of the rectangle, while the length is the longer side. This rectangle is also used to calculate the orientation angle of the grave outline. The poses of skeletons are classified with Resnet-152. For this, two classes have been defined: ‘supine’

and ‘flexed on one side’. 239 drawings of skeletons in supine position and 133 of skeletons flexed on one side were collected. They were all resized to 300x300 pixels to provide a uniform resolution. RMSProp was used as the optimizer with a learning rate of $1e-3$. It was trained 1000 epochs with a batch size of 16.

We identified several challenging constellations when using the aforementioned method on a wide variety of publications. Occasionally, objects are incorrectly assigned to a grave based on the distance. Often this is because multiple scales are present and the nearest scale belongs to an artefact instead of a grave. False negatives can also occur, leading other objects to be incorrectly grouped with a grave, such as north arrows belonging to different drawings.

A list of all graves in a publication is automatically generated once the process is complete. Each entry must subsequently be manually validated.

Graphical Interface

We designed and built a graphical user interface that allows manual correction of the annotations obtained through the automated process described above. Although our automatic approach is accurate for most publications, validation and potential manual correction by a domain expert are essential to maximise the reliability of our archaeological annotations. The graphical interface is a web application that is usable on a wide variety of devices including mobile devices. While we currently focus on drawings of graves, other types of objects such as ceramics could be analysed with minor modifications.

As our application follows an automated process and works by marking objects with their bounding boxes, it differs from other softwares commonly used to analyse drawings like CAD or image processing applications. It is also capable of performing basic statistical analysis for data visualisation purposes

The full semi-automated workflow for annotation consists of 6 distinct steps:

Step 1. Basic grave information. The ID assigned to the burial by the authors in the source publication is recorded. In case multiple images of the same grave are shown, the software will prevent duplicates in the results using this ID. In this step, the expert also has the option to discard drawings incorrectly classified as a grave.

Step 2. Correcting bounding boxes. The user can manually add, remove or change the bounding box assigned to a specific grave. Potential tasks include selecting a different scale on the page, resizing bounding boxes because they do not fully encapsulate an object or marking north arrows that were initially missed by object detection. During this step, a manual arrow has to be drawn for every skeleton following the spine and pointing towards the skull, which is necessary to determine the exact orientation of the skeleton in the grave. We will automate this procedure in the second release of our software. With the completion of this step, automated object detection is performed, analysing related objects and updating the existing database to reflect relevant changes performed through the manual input.

Step 3. Contour validation. The user is presented with all detected outlines to verify if they are correct. In case any issue arises, returning to the previous step is possible, to instead fit a manual bounding box around the grave or cross-section to indicate the width, length or depth. Fitting a manual bounding box removes the possibility to obtain the outside contour of this specific grave.

Step 4. Scale information. The next step is to validate the scale. The text indicating the real-world length of the scale has to be checked. Once this step is completed, all measurements are updated with the new scale information. In case no individual scale is provided and the publication uses a fixed scale, e.g. all drawings are 1:20, a different screen is shown. In this screen, the actual height of the

page (in cm) has to be entered manually together with the scale of the drawing. This way, all measurements can be calculated in the absence of a scale and the results are fully compatible with scaled publications.

Step 5. North arrow orientation. The angle of the north arrow can be adjusted manually based on a preview. In case an arrow is missing in the drawing, this screen will be skipped and size measurements and contours will still be collected without the orientation.

Step 6. Skeleton pose. Finally, the pose of all skeletons has to be validated, which can be either ‘unknown’, ‘flexed on the side’ or ‘supine’. As described above, a neural network will set the initial body position but it can be adjusted manually. Further positions could easily be added. ‘Unknown’ is used in cases where skeletal remains are visible but no body position can be discerned.

1.3 Results

Benchmarking

To evaluate performance and reliability of the software, we invited 10 participants to perform small computing tasks for 90 minutes at the Anthropology Institute, JGU Mainz. The only selection criterion for participants was that they had no prior experience with the AI software presented in this manuscript. The test group consisted of undergraduates, postgraduate and postdoctoral researchers from a variety of backgrounds, including archaeologists and non-archaeologists. They used an earlier version of our AI software *AutArch*, which did not yet include the multi-step guidance for the manual validation. All AI models were the same. Based on the experiment, we later made changes to the software.

None of the participants read Czech, as the catalogue used for the experiment was written in Czech and contained written descriptions of the burials in addition to the drawings ¹. Participants were divided into two groups. The first group began with *Inkscape* and then moved on to *AutArch*, while the second group began with *AutArch* and then moved to *Inkscape*. Both experiments were timed and limited to 30 minutes.

The two groups were given a very short induction to *Inkscape*. They were asked to import PDF pages containing graves from Dobeš and Limburský 2013 ¹, then manually measure each grave using the measuring function. A standard excel spreadsheet was provided with formulas to work out the actual size of graves based on the scale. We also gave a short introduction on how to use *AutArch*. They were asked to record the grave ID, make necessary corrections to the bounding boxes, draw arrows through the spines and validate the scales, arrows and the deposition type. The same publication ¹ had already been imported, and because the software did not yet include a guided process, a 12 step checklist was given to the participants.

The results of the experiment are shown in **figure 4**. Manually collected data and the participants’ *AutArch* results, i.e. width, length, etc., were compared to a baseline that we created using *AutArch* ourselves and the percentage deviation was recorded. The deviation of all values for a single grave was summed up and the average error was calculated between all graves for both *Inkscape* and *AutArch*. In instances where values were missing these specific values were skipped in the error calculation. Situations where certain values could not be obtained such as with missing cross sections were omitted. We observe that our AI-software (*AutArch*) produces considerably fewer errors (in % of the baseline) and is faster than manual recording using *Inkscape* (number of graves for each participant in a 30-minute window).

Despite the relatively low number of participants, this successfully demonstrates that our AI-assisted workflow performs significantly better than manual measurement using a drawing

software, i.e. is faster and a lot less prone to errors (**figure 4**). We expect this effect becomes more pronounced the longer these tasks are performed, due to the onset of mental fatigue.

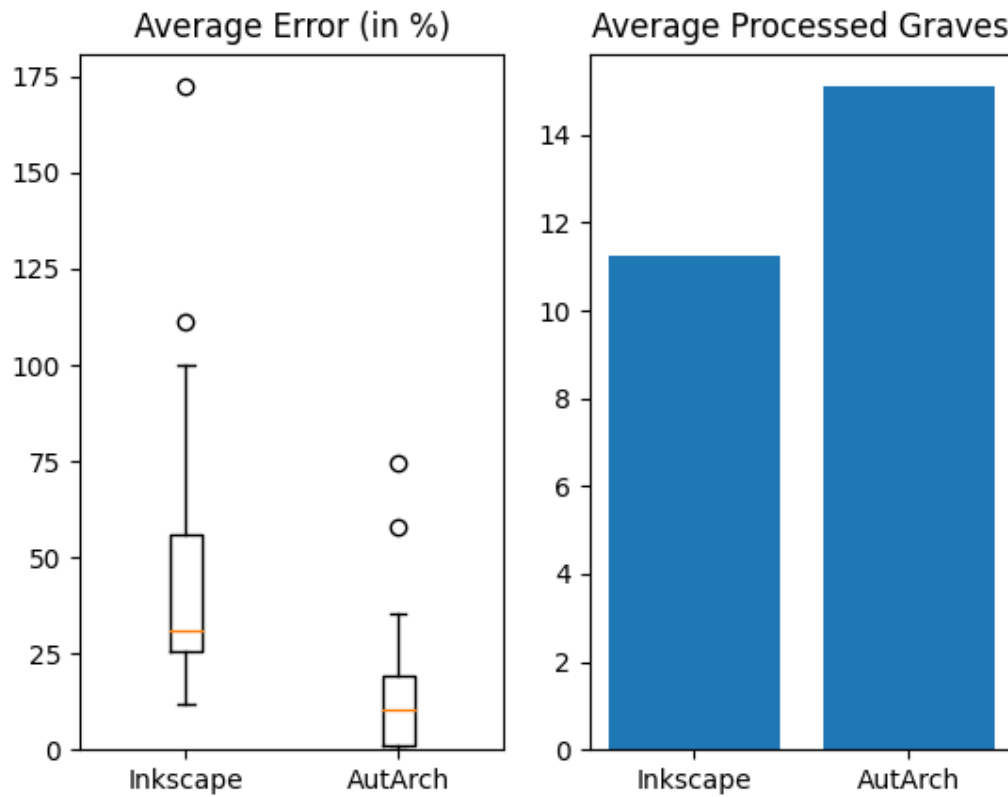


Figure 4. Benchmarking the method with ten users.

Practical applications

We analysed four different publications including the manual validation as a proof-of-concept ^{1,4,27,37}. The software is also capable of performing basic statistical analysis for data visualisation purposes. We compared the burials from Vlin  ves, which were attributed to the ‘Corded Ware’ culture with those attributed to the ‘Bell Beaker’. Our data shows clear differences in the orientation of the skeletons (**figure 5**). Interestingly, there are some deviations from the commonly described ‘east-west axis’ for ‘Corded Ware’ graves ³⁸ and north-south orientation for ‘Bell Beaker’ associated burials. We also generated a database of graves from four publications ^{1,4,27,37}, which has information about the width, length, depth, pit orientation of all burials and the number of skeletons with their orientation inside the grave.

Even though the full outlines of burial pits are an intermediate step to calculate their outside measurements, they also represent interesting data in themselves. Figure 6 shows the geometric whole-outlines of graves from their respective publications stacked over each other. Drawings that have no automatically detectable outline and use the manual bounding box instead are excluded here. We applied the methodology described in Matzig et al. 2021 ¹⁸ and modelled the outlines by EFDs (elliptic fourier descriptors) with 15 harmonics, projected on two dimensions with PCA (principal component analysis) (**figure 7**). Besides several outliers, the outlines of pit graves belonging to both

‘Corded Ware’ and ‘Bell Beaker’ were too similar to distinguish reasonable groups, underscoring their close cultural affinity ³⁹.

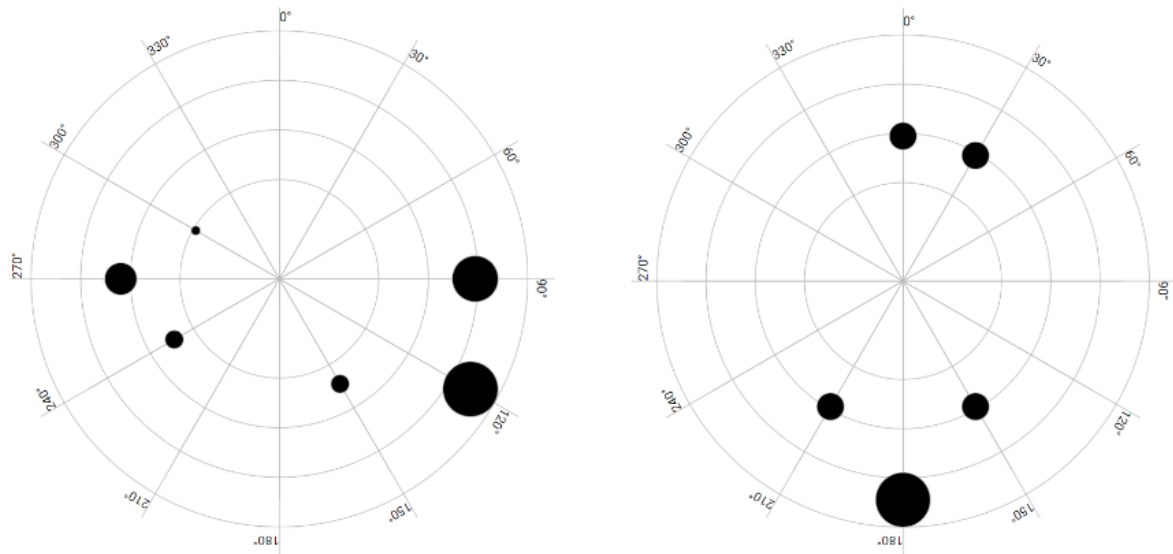
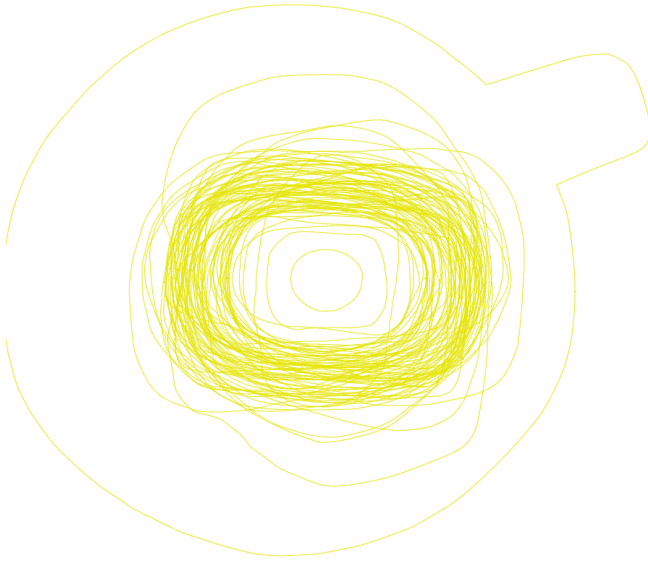
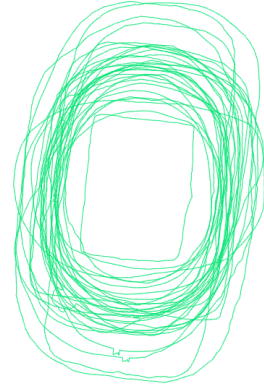


Figure 5. An example of numerical attribute that can be automatically retrieved using the AI-assisted workflow: the orientation of ‘Corded Ware’ ¹ (left, n = 39) and ‘Bell Beaker’ ²⁷ (right, n = 6) graves with skeletons from the site of Vliněves, Czech Republic.

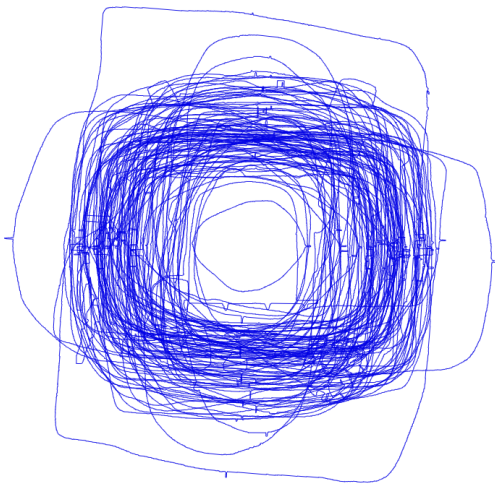
Vliněves 'Corded Ware' (n = 78)
Dobeš and Limburský 2013



Vliněves 'Bell Beaker' (n = 31)
Limburský 2012



Vikletice 'Corded Ware' (n = 102)
Buchvaldek & Koutecký 1970



Mondelange 'Bell Beaker' (n = 19)
Gazenbeek et al. 2009

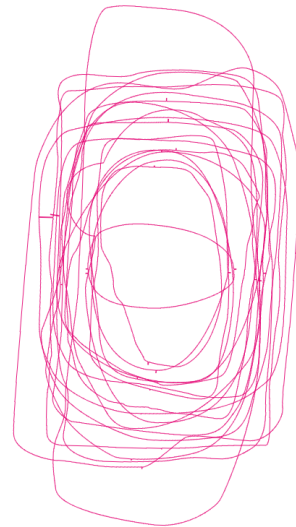


Figure 6. Shape variation (geometric 'whole-outlines'). Here grave outlines or cuts, retrieved through contour detection from four publications ^{1,4,27,37}, were automatically scaled and rotated using the AI-assisted workflow.

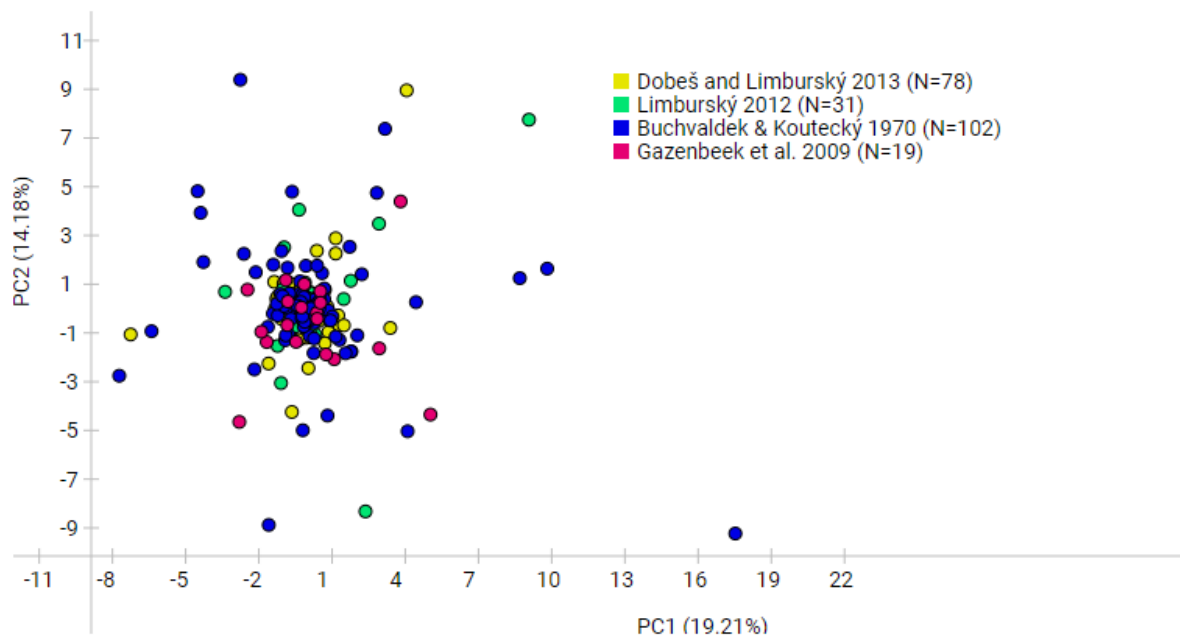


Figure 7. Geometric whole-outlines of graves using EFD (15 harmonics) projected on the first two principal components.

1.4 Discussion

Our approach provides a methodology to create a comparable and reproducible database with specific attributes such as the size of a burial. The current training dataset of just 391 is very small when compared to other commonly used datasets such as COCO⁴⁰. But even with such a limited training dataset, the model performs very well in detecting a variety of objects in archaeological publications. The automated detection of contours combined with EFD offers an alternative to landmark based geometric morphometrics¹⁸. The collection of material for this kind of analysis has been a time consuming task in the past, forcing researchers to normalise basic parameters such as size¹⁸, because scaling every single object was not practical. With our approach, we can harmonise the scales of every object to allow for meaningful comparisons. Furthermore, our database allows for complex, composite queries over all recorded attributes, e.g. burials within specific dimensions such as very small or very large graves, with specific orientations or with a certain number of skeletons among others can be obtained. The participants in our experiment were already proficient with our software after a few minutes only and produced annotations with considerably fewer errors compared to the manual approach (**figure 4**). We are confident that with the improvements implemented after our benchmark, new users will be able to use our software without extra time spent on training. Our participants created satisfying results, even though they had no prior experience in this field or with similar methods.

Limitations

Our current approach is limited by the level of detail and accuracy of the drawings themselves, i.e. information missing in the source material cannot be extracted. This may limit the set of attributes that can be collected e.g. for objects that do not have a clear outline. The current focus of our application emphasises the attributes associated with form and spatial relationships in the drawing. Applying our

method to other aspects of material culture, for instance ceramic ware, would require a broader set of attributes. These would include the fabric and surface treatment among many others. Published text might contain further information, but its analysis will be a future task.

Outlook

One unintended ethical risk of *AutArch* is the potential automation by AI of repetitive jobs such as database entry and curation, typically performed by paid trainees and technicians. This risk is present in all sectors where AI is being deployed. *AutArch* requires a human agent to manually validate database entries. In theory, the AI-assisted workflow should make the recording process significantly less tedious, freeing up time for more creative tasks like literature search and data analysis. In the future, skill sets may need to be altered to allow all researchers to work with new technology. There is huge potential to improve data collection in archaeology for other objects beyond graves including but not limited to buildings, ceramics, stone tools and arrowheads. Recording these objects is not limited to academic research but it could also be used for commercial archaeology and cultural heritage. Even large amounts of unpublished hand drawings could be analysed and added to the existing database. Our software uses well established high performance neural networks that work well with most existing hardware. Other more recent advances in machine learning such as Vision Transformers^{41–43} have greatly increased performance compared to Resnet-152 used in our application. Analysing the text of publications using established statistical NLP (natural language processing) or incorporating text into image classification using multi modal AI⁴⁴ provide opportunities for more efficient and extensive data collection. Besides the technical aspects, a new standard for documenting archaeological features such as graves might need to be created to ease integrations with software that can automatically digitise handwritten documentation.

1.5 Conclusions

In this paper we have presented a new method to tackle the challenge of large-scale archaeological data collection. Our approach improves speed and accuracy of manual methods, as shown by a benchmark experiment. We demonstrate the usefulness of the software by reproducing results on a small sample previously analysed manually. Furthermore, our shape related measurements of width, length and depth of burial pits are collected in a standardised manner. This allows to perform meta-analyses across different publications and to define and detect outliers with unusual shapes. Lastly, our approach increases the precision of measured angles to assess the orientation of skeletons and burial pits.

Acknowledgements

We thank Bianca Preda-Bălănică and Stefano Palalidis for their help with ‘Yamnaya’ references. We are also grateful to Miroslav Dobeš and Petr Limburský for the permission to reproduce illustrations from Vliněves. This research was supported by the German Science Foundation (DFG Project CO-MOVE, Grant n° 466680522, awarded to Maxime Brami). Volker Heyd's and Yoan Diekmann's contributions to this study were supported by the European Research Council (ERC) under the European Union's Horizon 2020 research and innovation program (Grant agreement n° 788616-YMPACT).

Supplementary Methodology

Convert PDF Pages to Images

Vips::Image.pdfload is used to convert the pdf files to single page images from ruby-vips 2.4.1⁴⁵ with libvips 8.9.1-2. Further pdf information such as the number of pages is obtained using pdf-reader 2.11.0⁴⁶.

Training Retinanet

The PyTorch 1.13.0 implementation of RetinaNet⁴⁷ using the network retinanet_resnet50_fpn_v2 was trained using 237 annotated pages containing drawings of burials, artefacts and text. Adam was used as the optimizer with an initial learning rate of 0.0001 and it was trained for 150 epochs. For the detection process, all objects with a confidence of lower than 80% were discarded. We classified the pages into the following classes: text, burial, skeleton, arrow, scale, grave cross section, ceramics, stone artefacts, artefacts (generic term for smaller items), shaft axe, table and map.

Grouping of Burials

A tree structure for every burial as its root was created from the output of the RetinaNet. All skeletons and grave goods inside the bounding box of the bounding box of the burial were assigned to the specific burial. The closest scale, north arrow and cross section were assigned based on the distance to a burial within a page. The distance was calculated using the Euclidean distance from the centre of the bounding boxes to other objects.

Contour Detection

We used findContours from OpenCV 4.5.2 with RETR_EXTERNAL and CHAIN_APPROX_SIMPLE to detect the outline of the burial, the north arrow, the cross section and the scale. The image was inverted, then converted to grayscale. After this step, threshold using the OpenCV threshold method with the parameters 40, 255 and THRESH_BINARY was performed. Then the largest contour was selected using the length of the arc. This outline was used to calculate the area, arc length, width, length and rotation of the burial. Area and arc length were retrieved using OpenCV contourArea and arcLength function. Width and length were created by first getting the bounding rectangle using minAreaRect. By definition, the width is the shorter side of the rectangle, length is the longer side of the rectangle. The angle is used from the bounding rectangle as well.

Spine Arrow

Spines were annotated manually using a directed arrow pointing towards the head of the skeleton. The angle was then calculated using this function:

$f(a_x, a_y, a_\alpha, s) = \text{atan}^2(a_x, a_y) - \text{atan}^2(-\sin(a_\alpha), -\cos(a_\alpha))$, with positive angles a ($a = a' + 360^\circ$ if $a' < 0^\circ$) mapped to the interval $[0, 1]$ by the transformation $a \frac{180}{\pi}$, where a_x and a_y are the x and y coordinate of the vector of the spine orientation arrow.

Training Dataset publications

Bader 1963⁴⁸, Bader & Khalikov 1976⁴⁹, Buchvaldek and Koutecky 1970³⁷, Comsa 1989⁵⁰, Dobeš & Limburský 2013¹, Dumitrescu 1980⁵¹, Frînculeasa 2013⁵², Frînculeasa et al. 2015²¹, Frînculeasa

et al. 2017 ⁵³, Frînculeasa et al. 2018 ⁵⁴, Frînculeasa 2019 ⁵⁵, Frînculeasa 2020 ⁵⁶, Frînculeasa et al. 2021 ⁵⁷, Frînculeasa et al. 2022 ⁵⁸, Gadzyackaya 1976 ⁵⁹, Gymashian 1993 ⁶⁰, Ivanova & Toshchev 2015 and references therein ⁶¹, Kostyleva & Utkin 2010 ⁶², Krainov 1963 ⁶³, Krainov 1964 ⁶⁴, Langova 2009 ²⁸, Limburský 2012 ²⁷, Lougas et al. 2007 ⁶⁵, Papac et al. 2021 ⁶⁶, Rosetti 1959 ⁶⁷, Toshchev, Shapovalov, Mikhailov 1991 and references therein ⁶⁸.

References

1. Dobeš, M. & Limburský, P. *Pohřebiště staršího eneolitu a šňůrové keramiky ve Vliněvsi*. vol. 22 (Vydal Archeologický ústav AV ČR, 2013).
2. Kristiansen, K. Towards a new paradigm? The third science revolution and its possible consequences in archaeology. *Curr. Swed. Archaeol.* **22**, 11–34 (2014).
3. Museum of London Archaeology Service. *Archaeological Site Manual*. (Museum of London, 1994).
4. Gazebeek, M. *et al.* *Mondelange (57, Moselle), 'PAC de la Sente', volume I: textes (Rapport final d'opération)*. (INRAP, 2009).
5. Ortolf, S. E. Das schnurkeramische Gräberfeld von Lauda-Königshofen im Taubertal. *Fundberichte Aus Baden-württemberg* **34**, 410–528 (2014).
6. Wentink, K. *Stereotype: The role of grave sets in corded ware and bell beaker funerary practices*. (Sidestone Press, 2020).
7. Gansell, A. R., Meent, J.-W. van de, Zairis, S. & Wiggins, C. H. Stylistic clusters and the Syrian/South Syrian tradition of first-millennium BCE Levantine ivory carving: a machine learning approach. *J. Archaeol. Sci.* **44**, 194–205 (2014).
8. Grosman, L., Karasik, A., Harush, O. & Smilansky, U. Archaeology in three dimensions: Computer-based methods in archaeological research. *J. East. Mediterr. Archaeol. Herit. Stud.* **2**, 48–64 (2014).
9. Hörr, C., Lindinger, E. & Brunnett, G. Machine learning based typology development in archaeology. *J. Comput. Cult. Herit.* **7**, 1–23 (2014).
10. Pawłowicz, L. M. & Downum, C. E. Applications of deep learning to decorated ceramic typology and classification: A case study using Tusayan White Ware from Northeast Arizona. *J. Archaeol. Sci.* **130**, 105375 (2021).
11. Berganzo-Besga, I., Orengo, H. A., Lumbreras, F., Aliende, P. & Ramsey, M. N. Automated detection and classification of multi-cell Phytoliths using Deep Learning-Based Algorithms. *J. Archaeol. Sci.* **148**, 105654 (2022).
12. Klassen, S., Weed, J. & Evans, D. Semi-supervised machine learning approaches for predicting the chronology of archaeological sites: A case study of temples from medieval Angkor, Cambodia. *PLoS One* **13**, e0205649 (2018).
13. Guyot, A., Hubert-Moy, L. & Lorho, T. Detecting Neolithic Burial Mounds from LiDAR-Derived Elevation Data Using a Multi-Scale Approach and Machine Learning Techniques. *Remote Sensing* **10**, 225 (2018).
14. Lambers, K., Verschoof-van der Vaart, W. B. & Bourgeois, Q. P. J. Integrating Remote Sensing, Machine Learning, and Citizen Science in Dutch Archaeological Prospection. *Remote Sensing* **11**, 794 (2019).
15. Wernke, S., VanValkenburgh, P. & Saito, A. Interregional Archaeology in the Age of Big Data: Building Online Collaborative Platforms for Virtual Survey in the Andes. *J. Field Archaeol.* **45**, S61–S74 (2020).
16. Lane Fox, A. H. On a Series of About Two Hundred Flint and Chert Arrowheads, Flakes, Thumbflints, and Borers, from the Rio Negro, Patagonia; with Some Remarks on the Stability of Form Observable in Stone Implements. *The Journal of the Anthropological Institute of Great Britain and Ireland* **4**, 311–323 (1875).
17. Resler, A., Yeshurun, R., Natalio, F. & Giryas, R. A deep-learning model for predictive archaeology and archaeological community detection. *Humanities and Social Sciences Communications* **8**, 1–10 (2021).
18. Matzig, D. N., Hussain, S. T. & Riede, F. Design Space Constraints and the Cultural Taxonomy of European Final Palaeolithic Large Tanged Points: A Comparison of Typological, Landmark-Based and Whole-Outline Geometric Morphometric Approaches. *Journal of Paleolithic Archaeology* **4**, 27 (2021).
19. Araujo, R. P. *et al.* Benchmarking methods and data for the whole-outline geometric morphometric analysis of lithic tools. *Evol. Anthropol.* **32**, 124–127 (2023).
20. Vander Linden, M. Le phénomène campaniforme dans l'Europe du 3ème millénaire avant notre

ère: synthèse et nouvelles perspectives. (2006).

21. Frînculeasa, A., Preda, B. & Heyd, V. Pit-Graves, Yamnaya and Kurgans along the Lower Danube: Disentangling IVth and IIIrd Millennium BC Burial Customs, Equipment and Chronology. *Praehistorische Zeitschrift* **90**, 45–113 (2015).
22. Kaiser, E. & Winger, K. Pit graves in Bulgaria and the Yamnaya Culture. *Praehistorische Zeitschrift* **90**, 114–140 (2015).
23. Furholt, M. Upending a ‘Totality’: Re-evaluating Corded Ware Variability in Late Neolithic Europe. *Proceedings of the Prehistoric Society* **80**, 67–86 (2014).
24. Nicolis, F. *Bell Beakers Today: Pottery, People, Culture, Symbols in Prehistoric Europe: Proceedings of the International Colloquium Riva Del Garda (Trento, Italy) 11-16 May 1998*. vol. 1 (Provincia autonoma di Trento, Servizio beni culturali, Ufficio beni archeologici, 2001).
25. Vander Linden, M. What linked the Bell Beakers in third millennium BC Europe? *Antiquity* **81**, 343–352 (2007).
26. Beckerman, S. M. *Corded ware coastal communities*. (Sidestone Press, 2015).
27. Limburský, P. *Pohřebišťe kultury se zvoncovitými poháry ve Vliněvsi : k problematice a chronologii konce eneolitu a počátku doby bronzové*. vol. 12 (Filozofická fakulta Univerzity Karlovy v Praze, 2012).
28. Langová, M. Výpověď objektů s lidskými kosterními pozůstatky na sídlišti únětické kultury ve Vliněvsi, okr. Mělník. (Univerzita Karlova, 2009).
29. Dobeš, M., Limburský, P. & Kyselý, R. Příspěvek k prostorovému uspořádání obytných areálů z konce středního eneolitu Rivnáčské osídlení ve Vlněvsi. *Archeologické* (2011).
30. Leong, M. C., Prasad, D. K., Lee, Y. T. & Lin, F. Semi-CNN Architecture for Effective Spatio-Temporal Learning in Action Recognition. *NATO Adv. Sci. Inst. Ser. E Appl. Sci.* **10**, 557 (2020).
31. Mao, A., Mohri, M. & Zhong, Y. Cross-Entropy Loss Functions: Theoretical Analysis and Applications. *arXiv [cs.LG]* (2023).
32. Ren, S., He, K., Girshick, R. & Sun, J. Faster R-CNN: Towards Real-Time Object Detection with Region Proposal Networks. *IEEE Trans. Pattern Anal. Mach. Intell.* **39**, 1137–1149 (2017).
33. He, K., Zhang, X., Ren, S. & Sun, J. Deep residual learning for image recognition. *and pattern recognition* (2016).
34. Suzuki, S. & Be, K. Topological structural analysis of digitized binary images by border following. *Computer Vision, Graphics, and Image Processing* **30**, 32–46 (1985).
35. Hinton, G., Srivastava, N. & Swersky, K. Neural Networks for Machine Learning. Preprint at https://www.cs.toronto.edu/~tijmen/csc321/slides/lecture_slides_lec6.pdf.
36. Structural Analysis and Shape Descriptors. Preprint at https://docs.opencv.org/4.x/d3/dc0/group__imgproc__shape.html#ga3d476a3417130ae5154aea421ca7ead9.
37. Buchvaldek, M. & Koutecký, D. *Vikletice: ein schnurkeramisches Gräberfeld*. vol. III (Universita Karlova, 1970).
38. Czebreszuk, J. Corded Ware from east to west. in *Ancient Europe 8000 BC - AD 1000. Encyclopedia of the Barbarian World* (eds. Bogucki, P. I. & Crabtree, P. J.) 467–474 (Thompson/Gale, 2004).
39. Furholt, M. Social Worlds and Communities of Practice: a polythetic culture model for 3rd millennium BC Europe in the light of current migration debates. *Préhistoires méditerr.* (2020) doi:10.4000/pm.2383.
40. Lin, T.-Y. et al. Microsoft COCO: Common Objects in Context. in *Computer Vision – ECCV 2014* 740–755 (Springer International Publishing, 2014).
41. Dosovitskiy, A. et al. An Image is Worth 16x16 Words: Transformers for Image Recognition at Scale. *arXiv [cs.CV]* (2020).
42. Dai, X. et al. Dynamic head: Unifying object detection heads with attentions. *arXiv [cs.CV]* 7373–7382 (2021).
43. Chen, Q. et al. Group DETR: Fast DETR training with group-wise one-to-many assignment. *arXiv [cs.CV]* 6633–6642 (2022).
44. Singh, A. et al. FLAVA: A foundational language and vision alignment model. *arXiv [cs.CV]* 15638–15650 (2021).

45. ruby-vips. Preprint at <https://github.com/libvips/ruby-vips>.
46. pdf-reader. Preprint at <https://github.com/yob/pdf-reader>.
47. PyTorch. Preprint at https://pytorch.org/vision/stable/models/generated/torchvision.models.detection.retinanet_resnet50_fpn_v2.html#torchvision.models.detection.retinanet_resnet50_fpn_v2.
48. Bader, O. N. *Балановский могильник: Из истории лесного Поволжья в эпоху бронзы*. (Издательство Академии наук СССР, 1963).
49. Bader, O. N. & Khalikov, A. K. *Памятники балановской культуры*. vol. вып. B1-25 (Археология СССР, 1976).
50. Comsa, E. Mormintele cu ocru din movila II - 1943 de la Ploiesti Triaj. *Thraco-Dacica* **10**, 181–188 (1989).
51. Dumitrescu, V. *The Neolithic Settlement at Rast:(south-west Oltenia, Romania)*. vol. 72 (BAR Publishing, 1980).
52. Frînculeasa, A. Podoabe preistorice din materiale vitroase. Descoperiri în cimitirul din epoca bronzului de la Câmpina (jud. Prahova). *Studii de Preistorie* 189–209 (2013).
53. Frînculeasa, A., Mirea, P. & Trohani, G. Local cultural settings and transregional phenomena: on the impact of a funerary ritual in the Lower Danube in the 4th millennium BC. *Buletinul Muzeului Județean Teleorman, Seria Arheologie* **9**, 75–116 (2017).
54. Frînculeasa, A., Preda, B., Simalcsik, A. & Negrea, O. Peisaje și contexte actuale: un tumul de pământ cercetat în localitatea Coada Izvorului, județul Prahova/Present landscapes and contexts: a burial mound excavated at Coada Izvorului, Prahova County. *Materiale și cercetări arheologice* **14**, 77–99 (2018).
55. Frînculeasa, A. The Children of the Steppe: descendance as a key to Yamnaya success. *Studii de Preistorie* 129–168 (2019).
56. Frînculeasa, A. Endangered monuments: in rescue of the mutilated and anonymous burial mounds of the steppe. *Revista de Arheologie, Antropologie și Studii Interdisciplinare* **2**, 41–79 (2020).
57. Frînculeasa, A., Negrea, O., Dîscă, C. & Simalcsik, A. Tumulul II de la Strejnicu (județul Prahova) – o prezentare arheologică și bio-antropologică. *Revista de Arheologie, Antropologie și Studii Interdisciplinare* **3**, 67–104 (2021).
58. Frînculeasa, A. *et al.* Ritualul Iamnaia și persistențe locale în prima jumătate a mileniului al III-lea (complexe funerare cercetate în anul 2021 în nordul Munteniei). *Revista de Arheologie, Antropologie și Studii Interdisciplinare (RAASI)* 127–165 (2022).
59. Gadzyackaya, O. S. *Памятники фатьяновской культуры: Ивановско-Горьковская группа*. vol. 1 (Наука, 1976).
60. Gymashian, C. V. Новые памятники каменного века Караби-Яйлы. in *Древности степного Причерноморья и Крыма 4* (eds. Toshchev, G. N., Shapovalov, G. I. & Mikhailov, B. D.) 3–9 (Запорожский Государственный Университет, 1993).
61. Ivanova, S. V. & Toshchev, G. N. ‘Буджанские Банки’ как маркеры: транскультурный и транстерриториальный аспект 1. *ССПК* **18**, (2015).
62. Костылева, Е. Л. & Уткин, А. В. *Нео-энеолитические могильники Верхнего Поволжья и Волго-Окского междуречья*. (Таус, 2010).
63. Krainov, D. A. *Памятники фатьяновской культуры: Московская группа*. vol. 1 (Изд-во Академии наук СССР, 1963).
64. Krainov, D. A. *Памятники фатьяновской культуры: Ярославско-Калининская группа*. (Изд-во ‘Наука’, 1964).
65. Lougas, L., Kriiska, A. & Maldre, L. New dates for the Late Neolithic Corded Ware Culture burials and early husbandry in the East Baltic region. *Archaeofauna* **16**, 21–31 (2007).
66. Papac, L. *et al.* Dynamic changes in genomic and social structures in third millennium BCE central Europe. *Sci Adv* **7**, (2021).
67. Rosetti, D. V. Movilele funerare de la Gurbănești (r. Lehliu, reg. București) / Les tumulus funéraires de Gurbănești. *Mater. și cercet. arheol.* **6**, 791–816 (1959).
68. *Древности Степного Причерноморья и Крыма II*. (Запорожский государственный университет, Запорожский областной краеведческий музей, 1991).